Computer Modeling in
Engineering & Sciences

Tech Science Press

Doi:10.32604/cmes.2025.063459

ARTICLE

Average Run Length in TEWMA Control Charts: Analytical Solutions for AR(p) Processes and Real Data Applications

Sirawit Makaew, Yupaporn Areepong* and Saowanit Sukparungsee

Department of Applied Statistics, King Mongkut's University of Technology North Bangkok, Bangkok, 10800, Thailand

*Corresponding Author: Yupaporn Areepong. Email: yupaporn.a@sci.kmutnb.ac.th

Received: 15 January 2025; Accepted: 01 April 2025; Published: 30 May 2025

ABSTRACT: This study aims to examine the explicit solution for calculating the Average Run Length (ARL) on the triple exponentially weighted moving average (TEWMA) control chart applied to autoregressive model (AR(p)), where AR(p) is an autoregressive model of order p, representing a time series with dependencies on its p previous values. Additionally, the study evaluates the accuracy of both explicit and numerical integral equation (NIE) solutions for AR(p) using the TEWMA control chart, focusing on the absolute percentage relative error. The results indicate that the explicit and approximate solutions are in close agreement. Furthermore, the study investigates the performance of exponentially weighted moving average (EWMA) and TEWMA control charts in detecting changes in the process, using the relative mean index (RMI) as a measure. The findings demonstrate that the TEWMA control chart outperforms the EWMA control chart in detecting process changes, especially when the value of λ is sufficiently large. In addition, an analysis using historical data from the SET index between January 2024 and May 2024 and historical data of global annual plastic production, the results of both data sets also emphasize the superior performance of the TEWMA control chart.

KEYWORDS: EWMA control chart; TEWMA control charts; average run length; shift detection; explicit formula; Fredholm integral equation; Banach's fixed-point theorem; AR(p) process

1 Introduction

The Fredholm integral equation plays a crucial role in various fields of mathematics and science, including physics, engineering mathematics, and signal analysis. It is a type of linear integral equation that can be categorized into two distinct forms: the first and the second kind. These two forms differ in structure and methods of solving them. One notable application of the second-kind Fredholm equation is in determining the Average Run Length (ARL) of control charts. The ARL is an important performance metric used to assess control charts, as it represents the average number of observations needed before a signal is triggered. The ARL has two key values: ARL0, which indicates the expected number of observations before a control chart detects that the process is out of control, and ARL1, which indicates the expected number of observations required when the process is actually out of control. Several methods have been proposed for calculating the ARL value of control charts, including approaches based on Markov chains, martingales, Monte Carlo simulations, explicit formulas, and numerical integral equations (NIEs). The Fredholm integral equation, characterized by a kernel function with constant integration limits, shares similarities with the Volterra integral equation, which has variable integration limits. The second kind of Fredholm integral equation is particularly significant in mathematical analysis and finds applications across various scientific fields. Solutions to these equations can be derived using iterative or analytical methods, with explicit formulas providing direct solutions for calculating the Average Run Length (ARL) [1,2]. Crowder [3] pioneered the application of second-kind Fredholm equations to EWMA charts, while Champ and Rigdon [4] extended this approach to the cumulative sum chart. Studies on explicit ARL formulas and numerical integral equations (NIEs) have since been conducted by several researchers [5–9], employing methods such as the midpoint, trapezoidal, Simpson's, Boole's, and Gauss-Legendre rules. For instance, Peerajit et al. [10] used the Gauss-Legendre quadrature to approximate ARL in CUSUM charts under long-memory processes, while Peerajit [11] applied NIEs to detect mean shifts in similar settings. Phanyaem [12] developed explicit formulas and NIEs for evaluating ARL of cumulative sum chart for a seasonal autoregressive with exogenous variable, ARX (P,r)L models, and Makaew et al. [13] utilized NIEs to analyze ARL for TEWMA charts in autoregressive processes. Peerajit [14] further applied NIEs for ARL approximation in EWMA charts for the fractionally integrated AR model with an exogenous variable (ARFIX) using the Gauss-Legendre quadrature. This study employs the trapezoidal rule for NIE approximations.

In Statistical Process Control (SPC), control charts are key tools for monitoring and maintaining process stability. Introduced by Shewhart [15], control charts visually track process data over time to detect trends or anomalies, ensuring consistency and quality. The Shewhart chart effectively identifies large shifts, while Page's [16] cumulative sum (CUSUM) chart is better suited for smaller shifts. Similarly, Robert [17] introduced the exponentially weighted moving average (EWMA) chart to enhance small-shift detection. Subsequent refinements include Shamma and Shamma [18] double EWMA (DEWMA) chart and Alevizakos et al.'s [19] triple EWMA (TEWMA) chart, designed for normally distributed data. Recent studies, such as those by Chatterjee [20,21], Supharakonsakun and Areepong [22], and Karoon et al. [23], have advanced ARL analysis for time series and moving average processes under these frameworks. Alevizakos et al. [24,25] further explored TEWMA charts, comparing various weighted moving average models to highlight the advantages of double, triple, and quadruple EWMA approaches. More recently, Hu et al. [26] proposed a Triple Exponentially Weighted Moving Average (TEWMA) control chart with a Variable Sampling Interval (VSI) feature to monitor the coefficient of variation (CV). Additional research on DEWMA and TEWMA control charts, as seen in [27–31], has further expanded the understanding and application of these charts in diverse quality control contexts.

Typically, EWMA and TEWMA control charts include both upper and lower control limits, making them essential tools for quality management. However, our research specifically focuses on one-sided criteria, specifically upper control limits. For manufacturing situations, the application of upper control limits has only shown its efficacy in the quick detection of production process problems. Companies can optimize resource allocation and provide consistent product quality by finding deviations from normal standards and tackling them before they escalate.

This study aims to develop an explicit formula for calculating the Average Run Length (ARL) of the autoregressive models of order p with exponential white noise under the TEWMA control chart framework. The existence and uniqueness of the solution will be demonstrated using Banach's fixed-point theorem and Hölder's inequality. Simulations will compare the performance of the explicit and NIE approaches for the TEWMA control chart, as well as evaluate the effectiveness of EWMA and TEWMA charts in detecting shifts in the AR(p) model. Finally, real-world data will be analyzed to assess the performance of both EWMA and TEWMA control charts for the AR(p) process.

2 Materials and Methods

The properties related to the AR(p) model, the EWMA control chart, and the TEWMA control chart are as follows.

2.1 Autoregressive Process

The Autoregressive (AR) process is a commonly used statistical tool for analyzing time series data. It forecasts the current value of a variable as a linear combination of its previous values (lags) along with a random error term. An AR model of order p, commonly written as AR(p), is described by the following equation:

$$X_t = \omega + \xi_1 X_{t-1} + \xi_2 X_{t-2} + \ldots + \xi_p X_{t-p} + \varepsilon_t, \tag{1}$$

where $\xi_i, \quad i = 1, 2, \ldots, p$ are coefficient parameters of the AR process $(|\xi_i| < 1)$, ω is the constant and ε_t is the error term of the model, which is distributed as an exponential white noise, $\varepsilon_t \sim Exp(\beta)$.

2.2 The EWMA Control Chart

The EWMA control charts are often used in quality control because they allow for the early detection of small changes in process performance. The EWMA control chart is defined as follows:

$$E_t = \lambda X_t + (1 - \lambda) E_{t-1}, \tag{2}$$

where λ is a parameter constrained within the range $0 < \lambda \leq 1$. Here, X_t represents the observations from the AR(p) process and $E_0 = \mu_0$ is defined as the initial value. The stop time for EWMA control charts is defined as follows:

$$\tau_h = \inf\{t > 0;\ E_t < g \ or \ E_t > h\}, \tag{3}$$

where g denotes the lower control limit, and h represents the upper control limit. The average run length (ARL) for the EWMA control chart on the AR(p) process, given an initial value of $E_0 = u$, is expressed as follows:

$$H(u) = ARL = E_\infty(\tau_h) \geq T, \quad E_0 = u, \tag{4}$$

where T represents a fixed constant and $E_\infty(.)$ denotes the expectation based on the assumption that observation ε_t follows the specified distribution. The mean and variance of the EWMA control chart are defined as $E(E_t) = \mu$ and $Var(E_t) = \left(\frac{\lambda}{2-\lambda}\right)\sigma^2$, respectively. The lower and the upper control limits for the EWMA control chart can be expressed as follows:

$$\begin{aligned} UCL &= \mu_0 + L_1\sigma\sqrt{\frac{\lambda}{(2-\lambda)}}, \\ LCL &= \mu_0 - L_1\sigma\sqrt{\frac{\lambda}{(2-\lambda)}}, \end{aligned} \tag{5}$$

where the mean and the standard deviation of the process are defined as μ_0, σ, respectively, and L_1 is a control width parameter.

2.3 The TEWMA Control Chart

One of the control charts developed from the EWMA control chart is the triple EWMA (TEWMA). The TEWMA control chart is defined as follows:

$$\begin{cases} E_t = \lambda X_t + (1-\lambda) E_{t-1}, \\ Y_t = \lambda E_t + (1-\lambda) Y_{t-1}, \\ TE_t = \lambda Y_t + (1-\lambda) W_{t-1}, \end{cases} \tag{6}$$

where λ is a parameter constrained within the range $0 < \lambda \leq 1$. Here, X_t represents observations from the AR(p) process. The initial value is given as $E_0 = Y_0 = TE_0 = \mu_0$. The stop time for the TEWMA control charts is defined as follows:

$$\tau_h = \inf\{t > 0;\ TE_t < g \ or \ TE_t > h\}, \tag{7}$$

where g denotes the lower control limit, and h represents the upper control limit. The average run length (ARL) for the TEWMA control chart on the AR(p) process, given an initial value of $TE_0 = u$, is expressed as follows:

$$H(u) = ARL = E_\infty(\tau_h) \geq T,\ \ TE_0 = u, \tag{8}$$

where T represents a fixed constant and $E_\infty(.)$ denotes the expectation based on the assumption that observation ε_t follows the specified distribution. The mean and variance of the EWMA control chart are defined as $E(TE_t) = \mu$, and $Var(TE_t) = \left(\frac{6(1-\lambda)^6\lambda}{(2-\lambda)^5} + \frac{12(1-\lambda)^4\lambda^2}{(2-\lambda)^4} + \frac{7(1-\lambda)^2\lambda^3}{(2-\lambda)^3} + \frac{\lambda^4}{(2-\lambda)^2}\right)\sigma^2$, respectively. The lower and the upper control limits for the TEWMA control chart can be expressed as follows:

$$\begin{aligned} UCL &= \mu_0 + L_2\sigma\sqrt{\frac{6(1-\lambda)^6\lambda}{(2-\lambda)^5} + \frac{12(1-\lambda)^4\lambda^2}{(2-\lambda)^4} + \frac{7(1-\lambda)^2\lambda^3}{(2-\lambda)^3} + \frac{\lambda^4}{(2-\lambda)^2}}, \\ LCL &= \mu_0 - L_2\sigma\sqrt{\frac{6(1-\lambda)^6\lambda}{(2-\lambda)^5} + \frac{12(1-\lambda)^4\lambda^2}{(2-\lambda)^4} + \frac{7(1-\lambda)^2\lambda^3}{(2-\lambda)^3} + \frac{\lambda^4}{(2-\lambda)^2}}, \end{aligned} \tag{9}$$

where the mean and the standard deviation of the process are defined as μ_0, σ, respectively, and L_2 is a control width parameter.

3 Explicit Formula for Solving the ARL

This section outlines the derivation of the explicit formula for the ARL of the TEWMA control chart applied to the AR model. The observations are assumed to follow an AR(p) process with exponentially distributed noise. The existence and uniqueness of the ARL solutions are then verified as detailed below. From Eq. (6), the recursive formula of TEWMA statistics can be written as follows:

$$TE_t = \lambda^3 X_t + \lambda^2(1-\lambda)E_{t-1} + \lambda(1-\lambda)Y_{t-1} + (1-\lambda)TE_{t-1} \tag{10}$$

Let X_t is observation on AR(p) model, then:

$$TE_t = \lambda^3\left[\omega + \sum_{i=1}^{p}\xi_i X_{t-p} + \varepsilon_t\right] + \lambda^2(1-\lambda)E_{t-1} + \lambda(1-\lambda)Y_{t-1} + (1-\lambda)TE_{t-1} \tag{11}$$

For $t = 1$, we obtain:

$$\begin{aligned} TE_1 &= \lambda^3\left[\omega + \sum_{i=1}^{p}\xi_i X_{1-p} + \varepsilon_1\right] + \lambda^2(1-\lambda)E_0 + \lambda(1-\lambda)Y_0 + (1-\lambda)TE_0 \\ &= M + \lambda^3\varepsilon_1 + (1-\lambda)u, \end{aligned}$$

where $M = \lambda^3\left[\omega + \sum_{i=1}^{p}\xi_i X_{1-p}\right] + \lambda^2(1-\lambda)E_0 + \lambda(1-\lambda)Y_0, 0 < \lambda \leq 1$ and $TE_0 = u$.

Consider a one-sided case for the in-control process, that is $0 \le TE_t \le h$, where $LCL = 0$ and $UCL = h$. So that, $0 \le M + \lambda^3 \varepsilon_1 + (1-\lambda)\, u \le h$.

Next, it rearranged into the form of ε_1, we get that:

$$\frac{-(1-\lambda)\, u - M}{\lambda^3} \le \varepsilon_1 \le \frac{h - (1-\lambda)\, u - M}{\lambda^3}$$

Based on the method introduced by Champ and Rigdon [4], derived from the second-kind Fredholm integral equation, the function $H(u)$ can be expressed as follows:

$$H(u) = 1 + \int_0^{\frac{h-(1-\lambda)u-M}{\lambda^3}} H\left[M + \lambda^3 y + (1-\lambda)\, u\right] f(y)\, dy \tag{12}$$

Let $W = M + \lambda^3 y + (1-\lambda)\, u$, then $y = \dfrac{W - (1-\lambda)\, u - M}{\lambda^3}$ and $dy = \dfrac{1}{\lambda^3} dW$. By changing the integral variable, Eq. (12) can be written as:

$$H(u) = 1 + \frac{1}{\lambda^3} \int_0^h H[W]\, f\left(\frac{W - (1-\lambda)\, u - M}{\lambda^3}\right) dW \tag{13}$$

Since $\varepsilon_1 \sim Exp(\beta)$, then $f(x) = \dfrac{1}{\beta} e^{-\frac{x}{\beta}};\ x \ge 0$. Thus:

$$H(u) = 1 + \frac{e^{\frac{(1-\lambda)u+M}{\beta\lambda^3}}}{\beta\lambda^3} \int_0^h H(w)\, e^{\frac{-W}{\beta\lambda^3}}\, dW. \tag{14}$$

Let $Q(u) = \dfrac{1}{\beta\lambda^3} e^{\frac{(1-\lambda)u+M}{\beta\lambda^3}}$ and $R = \int_0^h H(W)\, e^{\frac{-W}{\beta\lambda^3}}\, dW$, so that:

$$H(u) = 1 + Q(u)\, R \tag{15}$$

Consider that $R = \int_0^h H(W)\, e^{\frac{-W}{\beta\lambda^3}}\, dW$, then:

$$\begin{aligned} R &= \int_0^h H[W]\, e^{\frac{-W}{\beta\lambda^3}}\, dW \\ &= \int_0^h [1 + Q(W)\, R]\, e^{\frac{-W}{\beta\lambda^3}}\, dW \\ &= \int_0^h e^{\frac{-W}{\beta\lambda^3}}\, dW + \frac{R e^{\frac{M}{\beta\lambda^3}}}{\beta\lambda^3} \int_0^h e^{\frac{-W}{\beta\lambda^2}}\, dW \end{aligned}$$

So, we obtain $R = \dfrac{-\beta\lambda^3\left[e^{\frac{-h}{\beta\lambda^3}} - 1\right]}{1 + \frac{e^{\frac{M}{\beta\lambda^3}}}{\lambda}\left[e^{\frac{-h}{\beta\lambda^2}} - 1\right]}$.

Finally, by substituting R into Eq. (15), we obtain:

$$H(u) = 1 - \frac{e^{\frac{(1-\lambda)u+M}{\beta\lambda^3}}\left[e^{\frac{-h}{\beta\lambda^3}} - 1\right]}{\left(1 + \frac{e^{\frac{M}{\beta\lambda^3}}}{\lambda}\left[e^{\frac{-h}{\beta\lambda^2}} - 1\right]\right)} \tag{16}$$

Under the in-control condition ($\beta = \beta_0$), the explicit ARL_0 formula for the TEWMA control chart in an AR(p) process is given by:

$$ARL_0 = 1 - \frac{e^{\frac{(1-\lambda)u+M}{\beta_0\lambda^3}}\left[e^{\frac{-h}{\beta_0\lambda^3}} - 1\right]}{1 + \frac{e^{\frac{M}{\beta_0\lambda^3}}}{\lambda}\left[e^{\frac{-h}{\beta_0\lambda^2}} - 1\right]}.$$

When the process is out of control ($\beta = \beta_1,\ \ \beta_1 = (1+\delta)\,\beta_0$), where δ indicates the shift size, the explicit formula for ARL_1 in the TEWMA control chart for an AR(p) process is given by:

$$ARL_1 = 1 - \frac{e^{\frac{(1-\lambda)u+M}{\beta_1\lambda^3}}\left[e^{\frac{-h}{\beta_1\lambda^3}} - 1\right]}{1 + \frac{e^{\frac{M}{\beta_1\lambda^3}}}{\lambda}\left[e^{\frac{-h}{\beta_1\lambda^2}} - 1\right]}.$$

Proposition 1 Banach's Fixed-point Theorem: *Suppose that H defined on a complete metric space and $T: H \to H$ be a contraction mapping on H such that*:

$$\|T(H_1) - T(H_2)\| \le \delta\,\|H_1 - H_2\|$$

for:

$$H_1, H_2 \in H,$$

then the problem has a unique solution in H [32].

Proof: Let T be a contraction mapping operator defined as follows:

$$T(H(u)) = 1 + \frac{1}{\lambda^3}\int_0^n H(w)\,f\left(\frac{w-(1-\lambda)u-M}{\lambda^3}\right)dw,$$

for any $H_1, H_2 \in C[0,h]$ with $\|L\|_\infty = \sup_{u\in[0,b]} |H(u)|$. First, consider:

$$\begin{aligned}
&\|T(H_1(u)) - T(H_2(u))\|_\infty \\
&= \sup_{u\in[0,n]}\left\{\left|\left(1 + \frac{1}{\lambda^3}\int_0^n H_1(w)\,f\left(\frac{w-(1-\lambda)u-M}{\lambda^3}\right)dw\right) - \left(1 + \frac{1}{\lambda^3}\int_0^n H_2(w)\,f\left(\frac{w-(1-\lambda)u-M}{\lambda^3}\right)dw\right)\right|\right\} \\
&= \left|\frac{1}{\lambda^3}\int_0^n H_1(w)\,f\left(\frac{w-(1-\lambda)u-M}{\lambda^3}\right)dw - \frac{1}{\lambda^3}\int_0^n H_2(w)\,f\left(\frac{w-(1-\lambda)u-M}{\lambda^3}\right)dw\right| \\
&\le \frac{1}{\lambda^3}\int_0^n \|H_1(w) - H_2(w)\|_\infty\, f\left(\frac{w-(1-\lambda)u-M}{\lambda^3}\right)dw
\end{aligned}$$

Next, using the Hölder's Inequality, it can be written as follows:

$$\begin{aligned}
&\left\| T\left(H_1(u)\right) - T\left(H_2(u)\right)\right\|_{\infty} \\
&\le \frac{1}{\lambda^3}\left\|H_1 - H_2\right\|_{\infty} \int_0^n f\left(\frac{w-(1-\lambda)u-M}{\lambda^3}\right)dw \\
&\le \frac{1}{\lambda^3}\left\|H_1 - H_2\right\|_{\infty}\left(\int_0^n \left|f\left(\frac{w-(1-\lambda)u-M}{\lambda^3}\right)\right|^{\frac{1}{1-\sigma}} dw\right)^{1-\sigma}\left(\int_0^n |1|^{\frac{1}{\sigma}}dw\right)^{\sigma} \\
&\le \frac{n^{\sigma}}{\lambda^3}\left\|H_1 - H_2\right\|_{\infty}\left(\frac{e^{\frac{(1-\lambda)u-M}{\beta\lambda^3}}}{\beta\lambda^3}\right)^{1-\sigma}\left(\beta\lambda^3(1-\sigma)\left(1-e^{-\frac{n}{\beta\lambda^3(1-\sigma)}}\right)\right)^{1-\sigma} \\
&= \frac{n^{\sigma}}{\lambda^3}\left((1-\sigma)e^{\frac{(1-\lambda)u-M}{\beta\lambda^3}}\left(1-e^{-\frac{n}{\beta\lambda^3(1-\sigma)}}\right)\right)^{1-\sigma}\left\|H_1 - H_2\right\|_{\infty} \\
&\le \delta\left\|H_1 - H_2\right\|_{\infty},
\end{aligned}$$

where $\delta = \frac{n^{\sigma}}{\lambda^3}\left((1-\sigma)e^{\frac{(1-\lambda)u-M}{\beta\lambda^3}}\left(1-e^{-\frac{n}{\beta\lambda^3(1-\sigma)}}\right)\right)^{1-\sigma} \in [0,1)$, with $\sigma, \lambda \in (0,1)$, $\beta > 0$. From the assumption given above, therefore $\left\|T\left(H_1(u)\right) - T\left(H_2(u)\right)\right\| \le \delta\left\|H_1 - H_2\right\|_{\infty}$, then T is the contraction mapping on complete metric space, and by the Banach fixed point theorem, T has a unique solution in H. □

4 The NIE Method for Solving the ARL

The Numerical Integral Equation (NIE) method is employed to calculate the Average Run Length (ARL) for the TEWMA control chart on the AR(p) process. This method includes various techniques such as the Midpoint Rule, Trapezoidal Rule, and Simpson's Rule, etc. In this study, the trapezoidal rule is specifically utilized [13]. By approximating $L_{NIE}(u)$ through a system of m linear equations, the ARL is computed using the trapezoidal rule, as determined as follows:

$$L_{NIE}(u) \approx 1 + \frac{1}{\lambda^3}\sum_{j=1}^{m} w_j L\left(x_j\right)$$
$$f\left(\frac{x_j - (1-\lambda)u - \left(\lambda^3\left(\phi_0 + \phi_1 X_0 + \ldots + \phi_p X_{1-p}\right) + \lambda^2 Y_0(1-\lambda) + \lambda Z_0(1-\lambda)\right)}{\lambda^3}\right), \tag{17}$$

where $x_j = jw_j$, $w_j = \frac{h}{m}$, $j = 1, 2, \ldots, m-1$. Otherwise $w_j = \frac{h}{2m}$.

5 Simulated Results

In this section, the efficiency performance is compared between previously proposed approximations [11] and the explicit solution obtained in this study of TEWMA charts on AR models, specifically AR(1), AR(2), and AR(3) for the determination of the average run length (ARL), where a low ARL value indicates accurate detection efficiency. In the simulations, $ARL_0 = 370$ was considered. The approximation method used is the trapezoidal method with the number of iterations m = 1000. For the in-control process, the initial value is set to $\beta_0 = 10$. On the other hand for the out-of-control process, it is set to $\beta_1 = (1+\delta)\beta_0$, where δ is the shift size, which is considered from very small changes and then gradually moved as follows: 0.000, 0.001, .0003, 0.005, 0.007, 0.010, 0.030, 0.050, 0.070, 0.100, 0.300, 0.500, 0.700 and 1.000. Since we consider only one-sided, i.e., the upper control limit (UCL) = h and lower control limit (LCL) = 0. The coefficient parameters for the AR(1), AR(2), and AR(3) models were set as follows: $\xi_1 = 0.1$, $\xi_1 = \xi_2 = 0.1$ and $\xi_1 = \xi_2 = \xi_3 = 0.1$, respectively, with a constant (ω) set to 0. The steps of the process can be defined as follows:

Step 1: Specify ARL_0, λ and the constant (ω) and coefficient parameters $(\xi_i, i \geq 1)$ of AR(p) model.

Step 2: Specify the initial values of the process such as u, β_0, X_0.

Step 3: Calculate h for the explicit solution formula and the NIE formula.

Step 4: Calculate ARL_1 (out-of-control process) by using h from the previous step, consider $\beta_1 = (1 + \delta)\beta_0$, where δ is shift size.

The tool used to measure the efficiency of ARL between the estimated and the explicit solutions is measured by using the absolute percentage relative error (APRE). APRE is a measure of the accuracy of a forecast or estimate by comparing the predicted or estimated value to the actual value. APRE is calculated by finding the absolute error between the actual value and the predicted value, dividing the difference by the actual value and multiplying by 100 to express a percentage. The APRE formula is determined by:

$$APRE = \frac{|\text{Actual Value} - \text{Estimated Value}|}{\text{Actual Value}} \times 100$$

A comparison of the ARL of the explicit formula with the NIE method for the TEWMA control chart, when $\lambda = 0.15$, $\lambda = 0.75$ for the AR(1), AR(2), and AR(3), are shown in Tables 1–3, respectively. In each table, Time (sec) indicates the computation time of the method to find the NIE solution and the computation time of the explicit solution for every shift size (δ) value is less than 0.0001.

Table 1: Comparison of the ARL between the explicit and NIE solutions for the TEWMA control chart on AR(1) with $ARL_0 = 370$, given parameters $\omega = 0$, $\xi_1 = 0.1$, and $\beta_0 = 10$

$\lambda = 0.15$		$h = 1.846724 \times 10^{(-12)}$			$\lambda = 0.75$		$h = 6.5028756$		
δ	**Explicit**	**NIE**	**Time used**	**APRE (%)**	**δ**	**Explicit**	**NIE**	**Time used**	**APRE (%)**
0.000	370.000252	369.999998	<1.1870	0.0000687	0.000	370.001165	370.067934	<0.6400	0.0180455
0.001	358.911737	358.911954	<1.0780	0.0000605	0.001	296.031908	296.074549	<0.7500	0.0144041
0.003	337.786189	337.785861	<0.8600	0.000097	0.003	211.602626	211.624311	<0.6720	0.0102482
0.005	317.982471	317.982246	<1.0620	0.0000707	0.005	164.746714	164.759798	<0.7500	0.0079421
0.007	299.413968	299.413765	<1.2660	0.0000679	0.007	134.947608	134.956347	<0.8910	0.0064756
0.010	273.700709	273.700665	<1.2340	0.0000161	0.010	106.226223	106.2316	<0.8280	0.0050624
0.030	152.54171	152.541615	<1.2500	0.0000624	0.030	44.3231568	44.3240514	<0.7340	0.0020184
0.050	87.0868361	87.0869165	<1.1090	0.0000923	0.050	28.2842926	28.284641	<0.8290	0.0012318
0.070	50.9308514	50.9308403	<1.0460	0.0000218	0.070	20.9164952	20.9166775	<0.5470	0.0008716
0.100	23.8754908	23.8754797	<1.2660	0.0000465	0.100	15.1787325	15.1788224	<0.9690	0.0005923
0.300	1.3108621	1.3108623	<1.0630	0.0000153	0.300	5.8681721	5.8681812	<0.6560	0.0001551
0.500	1.0130207	1.0130207	<1.2180	0.0000000	0.500	3.9461889	3.9461917	<0.5620	0.000071
0.700	1.0011326	1.0011326	<1.2190	0.0000000	0.700	3.1154487	3.11545	<0.9220	0.0000417
1.000	1.000071	1.000071	<1.1880	0.0000000	1.000	2.4889253	2.4889259	<0.8910	0.0000241

Table 2: Comparison of the ARL between the explicit and NIE solutions for the TEWMA control chart on AR(2) with $ARL_0 = 370$, given parameters $\omega = 0$, $\xi_1 = \xi_2 = 0.1$, and $\beta_0 = 10$

$\lambda = 0.15$		$h = 1.828350 \times 10^{(-12)}$			$\lambda = 0.75$		$h = 6.3822473$		
δ	**Explicit**	**NIE**	**Time used**	**APRE (%)**	**δ**	**Explicit**	**NIE**	**Time used**	**APRE (%)**
0.000	370.000236	370.000242	<1.3590	0.0000016	0.000	370.001932	370.066114	<1.0320	0.0173463
0.001	358.90895	358.908616	<1.1560	0.0000931	0.001	294.559356	294.599937	<1.2340	0.0137771
0.003	337.776332	337.776011	<1.2030	0.0000951	0.003	209.365235	209.385641	<1.2810	0.0097469
0.005	317.966427	317.966686	<0.9690	0.0000812	0.005	162.500769	162.513006	<1.1100	0.0075301
0.007	299.393158	299.39322	<1.1720	0.0000207	0.007	132.848998	132.857139	<1.2340	0.0061278

(Continued)

Table 2 (continued)

λ = 0.15		h = 1.828350 × $10^{(-12)}$			λ = 0.75		h = 6.3822473		
δ	**Explicit**	**NIE**	**Time used**	**APRE (%)**	**δ**	**Explicit**	**NIE**	**Time used**	**APRE (%)**
0.010	273.673948	273.673846	<1.0470	0.0000373	0.010	104.381235	104.386226	<0.5940	0.0047815
0.030	152.497625	152.497583	<1.1250	0.000027	0.030	43.3942569	43.3950811	<0.9370	0.0018993
0.050	87.0459352	87.0459895	<1.2810	0.0000624	0.050	27.6743752	27.6746958	<0.7660	0.0011585
0.070	50.8982141	50.898219	<1.1560	0.0000096	0.070	20.4642241	20.4643918	<0.2820	0.0008195
0.100	23.8547127	23.8547084	<1.2190	0.000018	0.100	14.8539841	14.8540669	<0.7660	0.0005574
0.300	1.3101458	1.310146	<0.9840	0.0000153	0.300	5.7583563	5.7583647	<0.8440	0.0001459
0.500	1.0129774	1.0129774	<1.2190	0.0000000	0.500	3.8813431	3.8813458	<1.1250	0.0000696
0.700	1.001128	1.001128	<1.0160	0.0000000	0.700	3.0698278	3.069829	<0.9690	0.0000391
1.000	1.0000707	1.0000707	<1.3130	0.0000000	1.000	2.4575624	2.457563	<0.9530	0.0000244

Table 3: Comparison of the ARL between the explicit and NIE solutions for the TEWMA control chart on AR(3) with ARL_0 = 370 given parameters $\omega = 0$, $\xi_1 = \xi_2 = \xi_3 = 0.1$, and $\beta_0 = 10$

λ = 0.15		h = 1.846724 × $10^{(-12)}$			λ = 0.75		h = 6.5028756		
δ	**Explicit**	**NIE**	**Time used**	**APRE (%)**	**δ**	**Explicit**	**NIE**	**Time used**	**APRE (%)**
0.000	370.0003767	370.0001375	<0.7350	0.0000646	0.000	370.0065437	370.0682714	<0.7660	0.0166829
0.001	358.9048832	358.9049387	<0.7810	0.0000155	0.001	293.1210844	293.1597330	<0.7650	0.0131852
0.003	337.7660260	337.7658426	<0.7650	0.0000543	0.003	207.2017709	207.2209931	<0.6560	0.0092770
0.005	317.9506746	317.9508267	<0.7660	0.0000478	0.005	160.3417966	160.3532543	<0.6720	0.0071458
0.007	299.3726850	299.3723934	<0.6720	0.0000974	0.007	130.8392114	130.8468054	<0.5780	0.0058041
0.010	273.6470174	273.6467729	<1.1560	0.0000893	0.010	102.6206722	102.6253115	<0.5940	0.0045208
0.030	152.4534317	152.4534213	<0.6880	0.0000068	0.030	42.5143496	42.5151104	<0.5160	0.0017895
0.050	87.0049673	87.0050006	<0.8120	0.0000383	0.050	27.0974852	27.0977807	<0.9060	0.0010905
0.070	50.8655319	50.8655718	<1.0310	0.0000784	0.070	20.0366140	20.0367685	<0.8130	0.0007711
0.100	23.8339350	23.8339343	<0.8430	0.0000029	0.100	14.5469289	14.5470052	<0.7500	0.0005245
0.300	1.3094307	1.3094310	<0.6720	0.0000229	0.300	5.6541998	5.6542075	<0.4690	0.0001362
0.500	1.0129342	1.0129342	<0.6720	0.0000000	0.500	3.8196593	3.8196618	<0.6880	0.0000655
0.700	1.0011233	1.0011233	<1.0630	0.0000000	0.700	3.0263312	3.0263323	<0.5940	0.0000363
1.000	1.0000703	1.0000703	<1.0780	0.0000000	1.000	2.4275817	2.4275821	<0.8900	0.0000165

From the results in Tables 1–3, it can be seen that the explicit and approximate solutions have very close values for all the shift sizes from small to large changes, but the explicit solution is still superior in computation time for all the shift sizes. The performance of the TEWMA control chart was evaluated by comparing it to its prototype, the EWMA control chart, using the Relative Mean Index (RMI) [25] as a performance metric. RMI is a statistical tool designed to compare the central tendency of one dataset to another, typically a reference or standard value. It quantifies the relationship between the mean of a dataset and a reference value, offering insights into the chart's effectiveness. The RMI is calculated as follows:

$$\text{RMI} = \frac{1}{n}\sum_{i=1}^{n}\left[\frac{ARL_i\left(c\right) - ARL_i\left(s\right)}{ARL_i\left(s\right)}\right]$$

here, $ARL_i(c)$ represents the ARL of a control chart for a given shift size in row i, while $ARL_i(s)$ is the smallest ARL across all charts for the same row. A lower RMI value indicates superior performance in detecting shifts. Tables 4–6 present the comparison of ARL values for the EWMA and TEWMA control charts under various λ values (0.15, 0.50, and 0.75) applied to AR(1), AR(2), and AR(3) processes, respectively.

Table 4: Comparison of the ARL between the EWMA and TEWMA control charts on AR(1) with $ARL_0 = 370$, given parameters $\omega = 0$, $\xi_1 = 0.1$, and $\beta_0 = 10$

δ	$\lambda = 0.15$		$\lambda = 0.50$		$\lambda = 0.75$	
	EWMA $h = 1.602125$	**TEWMA** $h = 1.846724 \times 10^{(-12)}$	**EWMA** $h = 6.8104266$	**TEWMA** $h = 1.1373573$	**EWMA** $h = 13.5009086$	**TEWMA** h = 6.5028756
0.000	370.0038132	370.0002521	370.0039535	370.0026750	370.0023664	370.0011652
0.001	286.0255229	358.9117369	281.7410936	277.5636762	307.4425541	296.0319080
0.003	196.8346242	337.7861890	190.9147094	185.2101124	229.8375479	211.6026259
0.005	150.1305805	317.9824706	144.5050115	139.0655155	183.5886054	164.7467138
0.007	121.3949005	299.4139684	116.3318554	111.3891878	152.8857880	134.9476081
0.010	94.3786365	273.7007086	90.1044725	85.8489273	122.2862819	106.2262228
0.030	38.3121458	152.5417101	36.4600181	34.2762268	52.7311313	44.3231568
0.050	24.2498450	87.0868361	23.1645987	21.6344183	33.8558964	28.2842926
0.070	17.8542940	50.9308514	17.1359583	15.9228917	25.0623353	20.9164952
0.100	12.9037951	23.8754908	12.4744659	11.5180683	18.1608506	15.1787325
0.300	4.9498524	1.3108621	4.9665812	4.4708893	6.8721539	5.8681721
0.500	3.3369955	1.0130207	3.4207401	3.0471471	4.5358554	3.9461889
0.700	2.6501032	1.0011326	2.7506036	2.4418270	3.5287445	3.1154487
1.000	2.1400938	1.0000710	2.2427487	1.9931848	2.7720619	2.4889253
RMI	0.5612278	0.9807902	0.0684077	0.0000000	0.1336786	0.0000000

Table 5: Comparison of the ARL on the EWMA and TEWMA control charts for AR(2) with $ARL_0 = 370$, given parameters $\omega = 0$, $\xi_1 = \xi_2 = 0.1$, and $\beta_0 = 10$

δ	$\lambda = 0.15$		$\lambda = 0.50$	$\lambda = 0.75$		
	EWMA $h = 1.5848291$	**TEWMA** $h = 1.828350 \times 10^{(-12)}$	**EWMA** $h = 6.7137175$	**TEWMA** $h = 1.1230575$	**EWMA** $h = 13.220365$	**TEWMA** $h = 6.3822473$
0.000	370.0018183	370.0002364	370.0056426	370.0023091	370.0034833	370.0019317
0.001	285.5277840	358.9089498	280.6623956	276.9367207	305.6322898	294.5593557
0.003	196.1314322	337.7763322	189.4396929	184.3768204	226.8330458	209.3652345
0.005	149.4511410	317.9664274	143.1048834	138.2854024	180.4170894	162.5007694
0.007	120.7747826	299.3931576	115.0680466	110.6907283	149.8248096	132.8489980
0.010	93.8452894	273.6739483	89.0289901	85.2588430	119.5094815	104.3812354
0.030	38.0545427	152.4976245	35.9532682	34.0013958	51.2383649	43.3942569
0.050	24.0816418	87.0459352	22.8367144	21.4565395	32.8624001	27.6743752
0.070	17.7294489	50.8982141	16.8940832	15.7913779	24.3229582	20.4642241
0.100	12.8136883	23.8547127	12.3011497	11.4234270	17.6301954	14.8539841
0.300	4.9179042	1.3101458	4.9070576	4.4375195	6.6977892	5.7583563
0.500	3.3173513	1.0129774	3.3848878	3.0266949	4.4356103	3.8813431
0.700	2.6358288	1.0011280	2.7249309	2.4270120	3.4596853	3.0698278
1.000	2.1299073	1.0000707	2.2247054	1.9826584	2.7256967	2.4575624
RMI	0.5565128	0.9897406	0.0640659	0.0000000	0.1278382	0.0000000

Table 6: Comparison of the ARL on the EWMA and TEWMA control charts for AR(3) with $ARL_0 = 370$, given parameters $\omega = 0$, $\xi_1 = \xi_2 = \xi_3 = 0.1$, and $\beta_0 = 10$

δ	$\lambda = 0.15$		$\lambda = 0.50$		$\lambda = 0.75$	
	EWMA $h = 1.5677351$	**TEWMA** $h = 1.8101571 \times 10^{(-12)}$	**EWMA** $h = 6.6188845$	**TEWMA** $h = 1.1089803$	**EWMA** $h = 12.9501615$	**TEWMA** $h = 6.2653165$
0.000	370.0039363	370.0003767	370.0048233	370.0009573	370.0104975	370.0065437
0.001	285.0373327	358.9048832	279.6006371	276.3152799	303.8737840	293.1210844
0.003	195.4387669	337.7660260	188.0003670	183.5550249	223.9515511	207.2017709
0.005	148.7826890	317.9506746	141.7442239	137.5178437	177.3999237	160.3417966
0.007	120.1652168	299.3726850	113.8428423	110.0044477	146.9283959	130.8392114
0.010	93.3214584	273.6470174	87.9886628	84.6797651	116.8958676	102.6206722
0.030	37.8019451	152.4534317	35.4650999	33.7323183	49.8492475	42.5143496

(Continued)

Table 6 (continued)

δ	$\lambda = 0.15$		$\lambda = 0.50$		$\lambda = 0.75$	
	EWMA $h = 1.5677351$	**TEWMA** $h = 1.8101571 \times 10^{(-12)}$	**EWMA** $h = 6.6188845$	**TEWMA** $h = 1.1089803$	**EWMA** $h = 12.9501615$	**TEWMA** $h = 6.2653165$
0.050	23.9167374	87.0049673	22.5210569	21.2824567	31.9401247	27.0974852
0.070	17.6070435	50.8655319	16.6612368	15.6626817	23.6370482	20.0366140
0.100	12.7253205	23.8339350	12.1342562	11.3308078	17.1378958	14.5469289
0.300	4.8865147	1.3094307	4.8495669	4.4048279	6.5352413	5.6541998
0.500	3.2980256	1.0129342	3.3501756	3.0066413	4.3417334	3.8196593
0.700	2.6217733	1.0011233	2.7000288	2.4124765	3.3947825	3.0263312
1.000	2.1198683	1.0000703	2.2071690	1.9723239	2.6819472	2.4275817
RMI	0.5518756	0.9986229	0.0598956	0.0000000	0.1224334	0.0000000

From Tables 4–6, it can be seen that the TEWMA control chart is not suitable for considering the situation with small lambda, but when the lambda value increases, the efficiency of TEWMA will increase accordingly. Moreover, the comparison between TEWMA and EWMA control charts for different ARs shown in Tables 4–6 can be further explained with graphs as shown in Fig. 1 as follows.

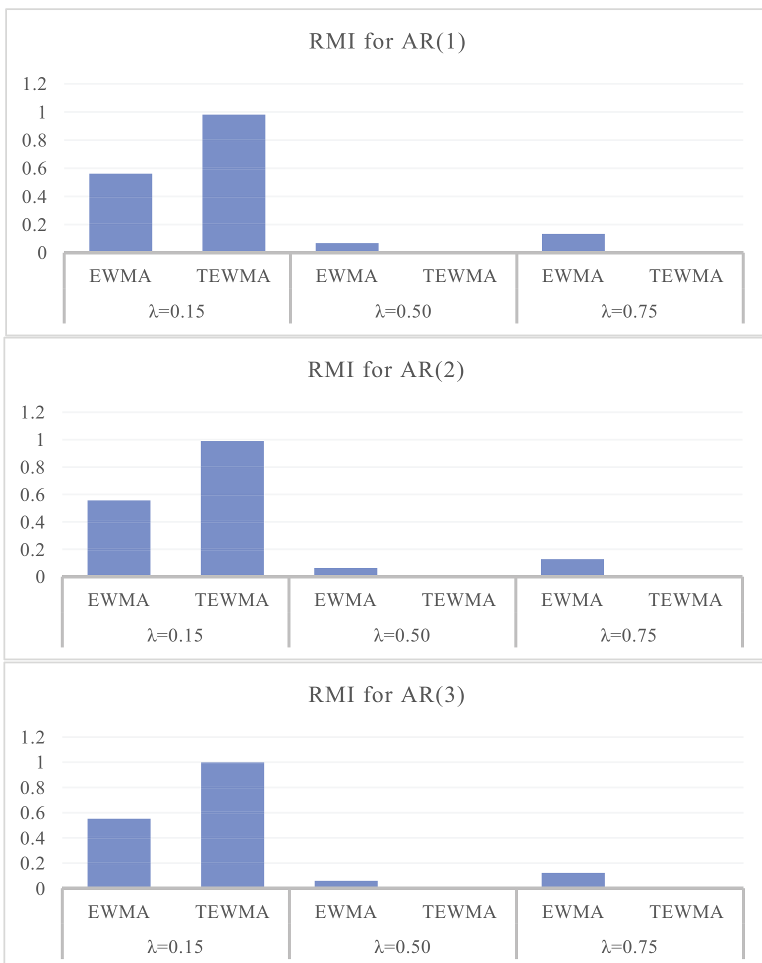

Figure 1: Consider RMI of EWMA and TEWMA control charts on various AR models for comparing performance when $\lambda = 0.15$, $\lambda = 0.50$ and $\lambda = 0.75$

6 Application to Real Data

This section compares TEWMA and EWMA control charts, starting with historical data from the SET index (January–May 2024). The compatibility of the dataset with AR models—AR(1), AR(2), and AR(3)—was evaluated based on Root Mean Squared Error (RMSE), Mean Absolute Percentage Error (MAPE), and Bayesian Information Criterion (BIC), as presented in Table 7. The AR(1) model, having the lowest RMSE and BIC values, was identified as the most suitable for this dataset. Additionally, the Kolmogorov-Smirnov Test was applied to confirm the suitability of white noise conforming to the exponential mean, as shown in Table 8. The SET index for the AR(1) model can be represented as follows:

$$X_t = 1382.234 + 0.918X_{t-1} + \varepsilon_t, \quad \varepsilon_t \sim Exp\,(6.8758)\,.$$

Table 7: Evaluation of the suitability of AR(1), AR(2), and AR(3) models

Model	RMSE	MAPE	BIC
AR(1)	10.126	0.497	4.722
AR(2)	10.158	0.495	4.774
AR(3)	10.210	0.494	4.830

Table 8: Testing the real data for exponential white noise of the exponential distribution

Model	Exponential parameter (β)	Kolmogorov-smirnov	Asymp Sig. (2-Tailed)
AR(1)	6.8758	0.751	0.626
AR(2)	7.0796	0.650	0.792
AR(3)	7.0592	0.657	0.780

Next, Table 9 presents the performance comparison between the EWMA and TEWMA control charts using previously determined real data from the AR(1) process. The steps of comparison of both control charts can be defined as follows:

Step 1: Specify ARL_0 and λ.

Step 2: The dataset was tested for fit with the AR model to find the constants and coefficient parameters of the model.

Step 3: Calculate h for the EWMA and the TEWMA control charts.

Step 4: Calculate ARL_1 (out-of-control process) of each control chart by using h from the previous step, consider $\beta_1 = (1 + \delta)\,\beta_0$, where δ is shift size.

From Table 9, the results are in accordance with the results in the simulation chapter, that is, the performance of TEWMA is not suitable considering a small lambda, but as the lambda increases, the performance of TEWMA will improve accordingly. In addition, Fig. 2 displays the RMI values of both control charts for AR(1), highlighting their comparative performance. Lastly, Fig. 3 illustrates the ARL values of the EWMA and TEWMA control charts for AR(1), showing the comparison across different parameters.

Table 9: Comparison of the ARL for the EWMA and TEWMA control charts on AR(1) with $ARL_0 = 370$, given parameters $\omega = 1382.234$, $\xi_1 = 0.918$, and $\beta_0 = 6.8758$

δ	$\lambda = 0.15$		$\lambda = 0.50$		$\lambda = 0.75$	
	EWMA h = 1.0052133	**TEWMA h = 0.000061907**	**EWMA h = 1.823065**	**TEWMA h = 0.1839268**	**EWMA h = 0.6629987**	**TEWMA h = 0.0703826**
0.000	370.0040028	370.0036706	370.0862742	370.0350660	370.1093046	370.0824437
0.001	297.9664911	365.3014136	232.8208345	238.3188195	177.3515115	142.4690294
0.003	214.4903906	356.1020820	133.9134074	139.3003270	87.1636696	64.1805653
0.005	167.5767476	347.1689151	94.1476356	98.4709965	57.9535362	41.5834155
0.007	137.5200286	338.4932970	72.6870727	76.1869639	43.5034196	30.8439484
0.010	108.3866385	325.9446797	54.2654302	56.9174793	31.7566154	22.3175448
0.030	45.0516978	254.7808559	20.5909620	21.3604840	11.7082524	8.1741398
0.050	28.5294375	201.0033149	12.9768761	13.2695713	7.4136571	5.2128511
0.070	20.9308750	159.9743760	9.6120831	9.6940981	5.5439054	3.9332920
0.100	15.0164924	115.3627372	7.0477050	6.9750953	4.1319447	2.9731937
0.300	5.4916217	19.4811314	2.9948016	2.7426744	1.9393195	1.5141437
0.500	3.5836669	5.7567474	2.1803784	1.9388595	1.5167249	1.2521796
0.700	2.7846064	2.6586148	1.8334757	1.6158800	1.3440174	1.1527595
1.000	2.2025871	1.4960857	1.5756284	1.3907677	1.2216251	1.0879078
RMI	0.0371160	2.3290378	0.0353303	0.0196603	0.3046227	0.0000000

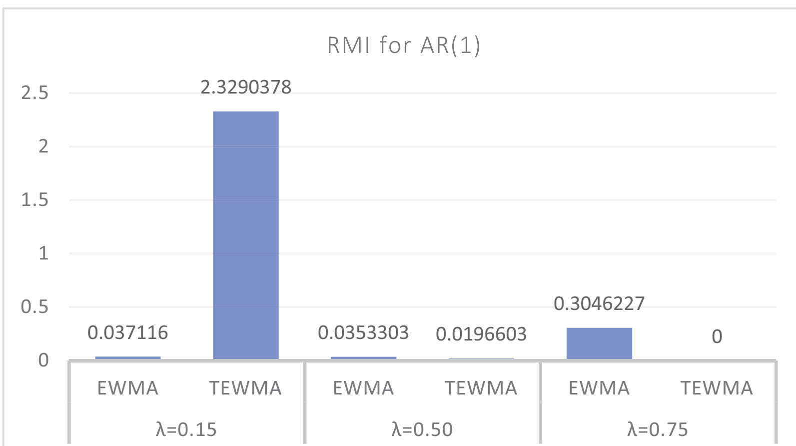

Figure 2: Consider RMI of EWMA and TEWMA control charts on AR(1) model for comparing performance when $\lambda = 0.15$, $\lambda = 0.50$ and $\lambda = 0.75$

From Fig. 3, it is found that the ARL value of the EWMA control chart will be higher than the TEWMA when considering the low lambda, but when the lambda value increases, the efficiency of TEWMA will increase until it is better than EWMA. Next, the performance comparison of the control charts between TEWMA and EWMA with historical data of annual global plastics production (1950–2019) is performed. Since we consider the model as AR(p), the dataset is checked for compatibility with different AR(p) models, and the exponential distribution of the error terms is examined as follows.

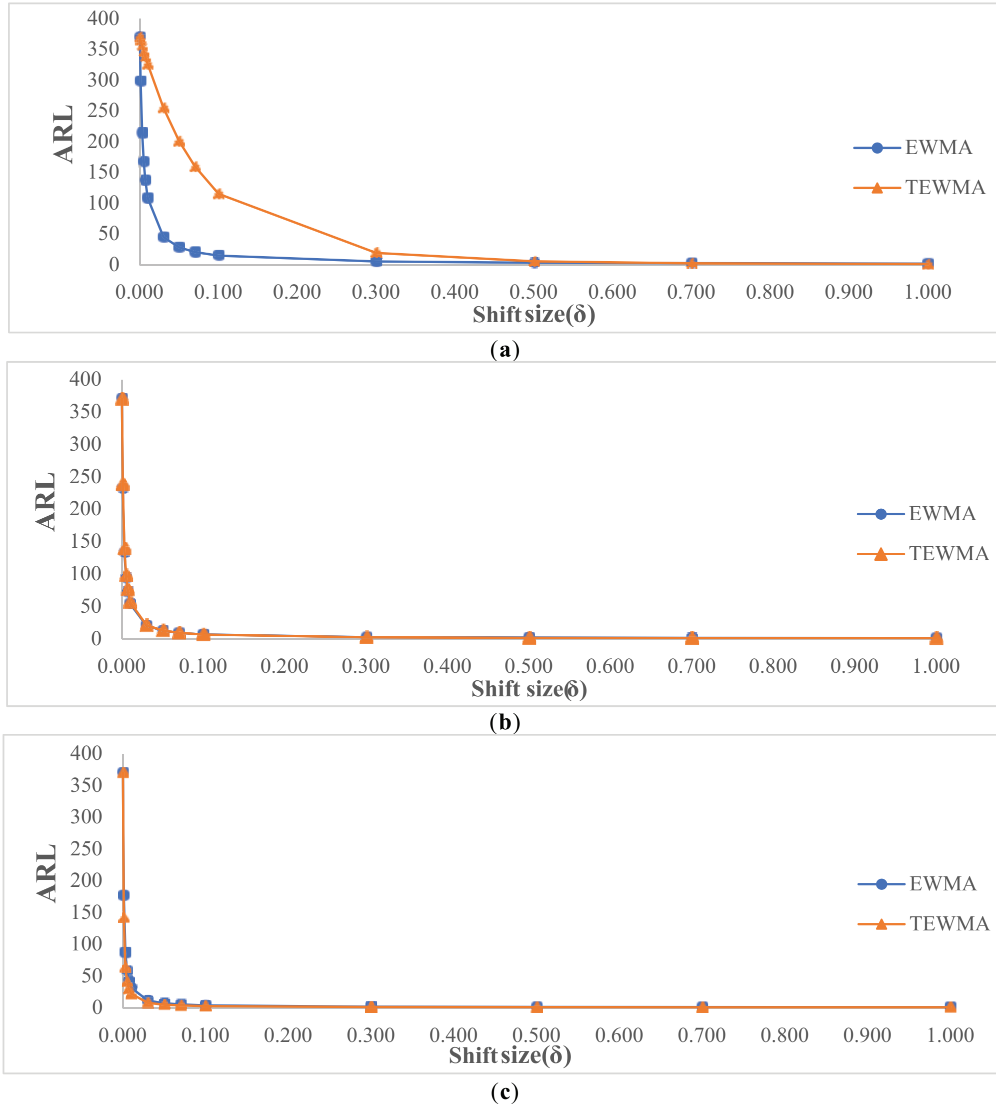

Figure 3: Comparison of the ARL between the TEWMA and the EWMA control charts for (**a**) $\lambda = 0.15$, (**b**) $\lambda = 0.50$, and (**c**) $\lambda = 0.75$

From Tables 10 and 11, it is found that the data set is most compatible with the AR(1) model, and the error term has an exponential distribution which can be written as follows:

$$Y_t = 137563820.884 + 0.999\ Y_{t-1} + \varepsilon_t, \quad \varepsilon_t \sim Exp\,(7834147.726)\,.$$

Table 10: Evaluation of the suitability of AR(1), AR(2), and AR(3) models

Model	RMSE	MAPE	BIC
AR(1)	19133381.711	106.024	33.657
AR(2)	19421286.316	106.183	33.748
AR(3)	19504089.239	106.103	33.818

Table 11: Testing the real data for exponential white noise of the exponential distribution

Model	Exponential parameter (β)	Kolmogorov-smirnov	Asymp Sig. (2-Tailed)
AR(1)	7834,147.726	0.958	0.318
AR(2)	8091,190.908	0.945	0.334
AR(3)	7970,542.372	0.949	0.329

Next, Table 12 presents the performance comparison between the EWMA and TEWMA control charts using previously determined real data from the AR(1) process. In addition, Fig. 3 displays the RMI values of both control charts for AR(1), highlighting their comparative performance.

Table 12: Comparison of the ARL for the EWMA and TEWMA control charts on AR(1) with $ARL_0 = 370$, given parameters $\omega = 137563820.884$, $\xi_1 = 0.999$, and $\beta_0 = 7834147.726$

δ	$\lambda = 0.15$		$\lambda = 0.50$		$\lambda = 0.75$	
	EWMA h = 0.02772733	**TEWMA h = 0.0006238612**	**EWMA h = 0.09242445**	**TEWMA h = 0.023106092**	**EWMA h = 0.1386367**	**TEWMA h = 0.07798308**
0.000	370.0517955	370.0067866	370.0747139	370.0063494	370.0995347	370.0008681
0.001	47.5662790	47.5667289	47.5666205	47.5655243	47.5669996	47.5654123
0.003	17.6803649	17.6807552	17.6804044	17.6802617	17.6804542	17.6802426
0.005	11.0282293	11.0284940	11.0282439	11.0281916	11.0282629	11.0281836
0.007	8.1014722	8.1016672	8.1014787	8.1014525	8.1014884	8.1014474
0.010	5.8770968	5.8772352	5.8770993	5.8770864	5.8771039	5.8770834
0.030	2.3843143	2.3843547	2.3843141	2.3843129	2.3843146	2.3843123
0.050	1.6995719	1.6995921	1.6995718	1.6995714	1.6995719	1.6995711
0.070	1.4194280	1.4194398	1.4194279	1.4194277	1.4194279	1.4194275
0.100	1.2250719	1.2250780	1.2250718	1.2250717	1.2250718	1.2250716
0.300	1.0135166	1.0135169	1.0135166	1.0135166	1.0135166	1.0135166
0.500	1.0019123	1.0019124	1.0019123	1.0019123	1.0019123	1.0019123
0.700	1.0004251	1.0004251	1.0004251	1.0004251	1.0004251	1.0004251
1.000	1.0000767	1.0000767	1.0000767	1.0000767	1.0000767	1.0000767
RMI	0.0000087	0.0000104	0.0000162	0.0000000	0.0000235	0.0000000

From Table 12, it can be seen that the results have the same direction as the results from the previous dataset when considering the RMI values. Then, to make it clearer, it is shown by the RMI values in Fig. 4.

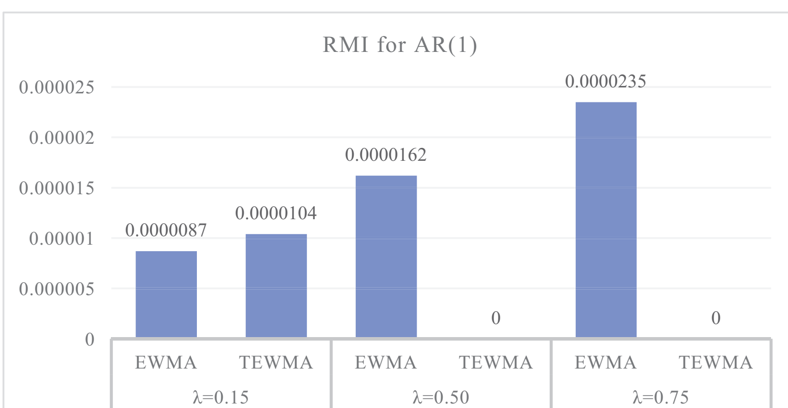

Figure 4: Consider RMI of EWMA and TEWMA control charts on AR(1) model for comparing performance when $\lambda = 0.15$, $\lambda = 0.50$ and $\lambda = 0.75$

7 Conclusion

This study evaluates the performance of control charts based on ARL. Both the explicit solution method and the numerical integral equation (NIE) method were applied to TEWMA control charts for various AR processes with exponential white noise. The efficiency of these methods was assessed in terms of APRE and computation time. The simulation results indicate that although both methods give similar results, the proposed explicit solution is less computationally intensive than the NIE method for all shift sizes. The performance of the TEWMA control chart was further compared to the EWMA control chart across different AR processes using RMI values. The results revealed that although the TEWMA chart is less effective for small λ, it outperforms the EWMA chart in detecting shifts across all shift sizes. Additionally, the comparison of TEWMA and EWMA charts was extended to real-world data, specifically the historical data of the SET index and historical data of annual global plastics production. The findings confirm that the TEWMA chart demonstrates superior performance in detecting changes compared to the EWMA chart for most λ values, consistent with the simulation results. However, a limitation of this study is that the TEWMA control chart may not perform well with small λ values, i.e., if small λ values are to be considered, the EWMA control chart is more suitable. Future research will focus on exploring TEWMA control charts or other types of control charts under different processes.

Acknowledgement: The authors confirm that this research was conducted independently by the listed authors, with no external contributors involved in any stage of the study.

Funding Statement: This research budget was allocated by the National Science, Research and Innovation Fund (NSRF), and King Mongkut's University of Technology North Bangkok under contract no. KMUTNB-FF-68-B-08.

Author Contributions: Conceptualization, Sirawit Makaew and Yupaporn Areepong; validation, Yupaporn Areepong; methodology, Sirawit Makaew and Saowanit Sukparungsee; software, Sirawit Makaew; formal analysis, Sirawit Makaew and Saowanit Sukparungsee; investigation, Yupaporn Areepong; resources, Yupaporn Areepong; data curation, Sirawit Makaew; writing—original draft preparation, Yupaporn Areepong and Saowanit Sukparungsee; writing—review and editing, Sirawit Makaew and Yupaporn Areepong; visualization, Yupaporn Areepong; supervision, Yupaporn Areepong; funding acquisition, Yupaporn Areepong. All authors reviewed the results and approved the final version of the manuscript.

Availability of Data and Materials: The datasets used in this study are publicly available. The historical data from the SET index (January–May 2024) can be accessed at https://th.investing.com/indices/thailand-set. The historical data on annual global plastics production (1950–2019) is available at https://ourworldindata.org/grapher/global-plastics-production (accessed on 1 January 2025). No additional datasets were generated or analyzed during the study.

Ethics Approval: Not applicable.

Conflicts of Interest: The authors declare no conflicts of interest to report regarding the present study.

References

1. Knoth S, Saleh NA, Mahmoud MA, Woodall WH, Tercero-Gómez VG. A critique of a variety of "memory-based" process monitoring methods. J Qual Technol. 2023;55(1):18–42. doi:10.1080/00224065.2022.2034487.
2. Li Z, Zou C, Gong Z, Wang Z. The computation of average run length and average time to signal: an overview. J Stat Comput Simul. 2014;84(8):1779–802. doi:10.1080/00949655.2013.766737.
3. Crowder SV. A simple method for studying run-length distributions of exponentially weighted moving average charts. Technometrics. 1987;29(4):401–7.

4. Champ CW, Rigdon SE. A comparison of the markov chain and the integral equation approaches for evaluating the run length distribution of quality control charts. Commun Stat-Simul Comput. 1991; 20(1):191–204. doi:10.1080/03610919108812948.
5. Mititelu G, Areepong Y, Sukparungsee S, Novikov A. Explicit analytical solutions for the average run length of CUSUM and EWMA charts. East-West J Math. 2010;12:253–65.
6. Raweesawat K, Sukparungsee S. Explicit formula of ARL for SMA $(Q)_L$ with exponential white noise on EWMA control chart of ZIPINAR model with an excessive number of zeros. Appl Sci Eng Prog. 2022;15(3):4588.
7. Chang YM, Wu TL. On average run lengths of control charts for autocorrelated processes. Methodol Comput Appl Probab. 2011;13(2):419–31.
8. Demirkol Akyol S, Bayhan M. ARL performances of control charts for autocorrelated data. In: Proceedings of the 38th International Conference on Computers and Industrial Engineering; 2008 Oct 31–Nov 2; Beijing, China. p. 400–8.
9. Petcharat K. Explicit formula of ARL for SMA $(Q)_L$ with exponential white noise on EWMA chart. Int J Appl Phys Math. 2016;6(4):218–25.
10. Peerajit W, Areepong Y, Sukparungsee S. Numerical integral equation method for ARL of CUSUM chart for long-memory process with non-seasonal and seasonal ARFIMA models. Thail Stat. 2018;16(1):26–37.
11. Peerajit W. An approximation to the average run length on a CUSUM control chart with a numerical integral equation method for a long-memory ARFIMAX model. J Appl Sci Emerg Technol. 2020;19(2):37–51.
12. Phanyaem S. Explicit formulas and numerical integral equation of ARL for $SARX(P,r)_L$ model based on CUSUM chart. Math Stat. 2022;10(1):88–99.
13. Makaew S, Areepong Y, Sukparungsee S. Numerical integral equation methods of average run length on triple EWMA control chart for autoregressive process. In: 2023 Research, Invention, and Innovation Congress: Innovative Electricals and Electronics (RI2C); 2023 Aug 24–25; Bangkok, Thailand. p. 216–9.
14. Peerajit W. Approximating the ARL to monitor small shifts in the mean of an AR fractionally integrated with an exogenous variable process running on an EWMA control chart. WSEAS Trans Syst. 2024;23:1–10.
15. Shewhart WA. Quality control charts. Bell Syst Tech J. 1926;5(4):593–603.
16. Page ES. Continuous inspection schemes. Biometrika. 1954;41(1–2):100–15.
17. Roberts SW. Properties of control chart zone tests. Bell Syst Tech J. 1958;37(1):83–114.
18. Shamma SE, Shamma AK. Development and evaluation of control charts using double exponentially weighted moving averages. Int J Qual Reliab Manag. 1992;9(6):18–25. doi:10.1108/02656719210018570.
19. Alevizakos V, Chatterjee K, Koukouvinos C. The triple exponentially weighted moving average control chart. Qual Technol Quant Manag. 2020;18(3):326–54. doi:10.1080/16843703.2020.1809063.
20. Chatterjee K, Koukouvinos C, Lappa A. A new double exponentially weighted moving average control chart for monitoring both location and dispersion. Qual Reliab Eng Int. 2022;38(4):1687–712. doi:10.1002/qre.3046.
21. Chatterjee K, Koukouvinos C, Lappa A. Monitoring process mean and variability with one triple EWMA chart. Commun Stat-Simul Comput. 2022;53(2):611–41. doi:10.1080/03610918.2022.2025835.
22. Supharakonsakun Y, Areepong Y. ARL evaluation of a DEWMA control chart for autocorrelated data: a case study on prices of major industrial commodities. Emerg Sci J. 2023;7(5):1771–86. doi:10.28991/ESJ-2023-07-05-020.
23. Karoon K, Areepong Y, Sukparungsee S. Modification of ARL for detecting changes on the double EWMA chart in time series data with the autoregressive model. Connect Sci. 2023;35(1):2219040. doi:10.1080/09540091.2023.2219040.
24. Alevizakos V, Chatterjee K, Koukouvinos C. A triple exponentially weighted moving average control chart for monitoring time between events. Qual Reliab Eng Int. 2021;37(3):1059–79. doi:10.1002/qre.2781.
25. Alevizakos V, Chatterjee K, Koukouvinos C. On the performance and comparison of various memory-type control charts. Commun Stat-Simul Comput. 2024. 1–21. doi:10.1080/03610918.2024.2310692.
26. Hu X, Zhang S, Xie F, Song Z. Triple exponentially weighted moving average control charts without or with variable sampling interval for monitoring the coefficient of variation. J Stat Comput Simul. 2023;94(3):536–70. doi:10.1080/00949655.2023.2262072.

27. Alevizakos V, Chatterjee K, Koukouvinos C. Modified EWMA and DEWMA control charts for process monitoring. Commun Stat-Theory Methods. 2021;51(21):7390–412. doi:10.1080/03610926.2021.1872642.
28. Alevizakos V, Chatterjee K, Koukouvinos C. Nonparametric triple exponentially weighted moving average signed-rank control chart for monitoring shifts in the process location. Qual Reliab Eng Int. 2021;37(8):2622–45. doi:10.1002/qre.2879.
29. Raza MA, Nawaz T, Aslam M, Bhatti SH, Sherwani RAK. A new nonparametric double exponentially weighted moving average control chart. Qual Reliab Eng Int. 2020;36(1):68–87. doi:10.1002/qre.2560.
30. Alevizakos V, Koukouvinos C, Chatterjee K. A nonparametric double generally weighted moving average signed-rank control chart for monitoring process location. Qual Reliab Eng Int. 2020;36(7):2441–58. doi:10.1002/qre.2706.
31. Alevizakos V, Koukouvinos C. Monitoring of zero-inflated binomial processes with a DEWMA control chart. J Appl Stat. 2020;48(7):1319–38. doi:10.1080/02664763.2020.1761950.
32. Kreyszig E. Introductory functional analysis with applications. Hoboken, NJ, USA: John Wiley & Sons, Inc.; 1989.